A novel behavioral paradigm using mice to study predictive postural control

Yurika Doi[1,2], Meiko Asaka[3], Richard T. Born[2,4], Dai Yanagihara[3,5], Naoshige Uchida[1,6,*]

[1] Department of Molecular and Cellular Biology, Harvard University, Cambridge, MA, USA

[2] Program in Neuroscience, Harvard Medical School, Boston, MA, USA

[3] Cognition and Behavior Joint Research Laboratory, RIKEN center for Brain Science, Wako, Japan

[4] Department of Neurobiology, Harvard Medical School, Boston, MA, USA

[5] Department of Life Sciences, Graduate School of Arts and Sciences, The University of Tokyo, Tokyo, Japan

[6] Center for Brain Science, Harvard University, Cambridge, MA, USA

[*] Corresponding author

Email: uchida@mcb.harvard.edu

Abstract

Postural control circuitry performs the essential function of maintaining balance and body position in response to perturbations that are either self-generated (e.g. reaching to pick up an object) or externally delivered (e.g. being pushed by another person). Human studies have shown that anticipation of predictable postural disturbances can modulate such responses. This indicates that postural control could involve higher-level neural structures associated with predictive functions, rather than being purely reactive. However, the underlying neural circuitry remains largely unknown. To enable studies of predictive postural control circuits, we developed a novel task for *mice*. In this task, modeled after human studies, a dynamic platform generated reproducible translational perturbations. While mice stood bipedally atop a perch to receive water rewards, they experienced backward translations that were either unpredictable or preceded by an auditory cue. To validate the task, we investigated the effect of the auditory cue on postural responses to perturbations across multiple days in three mice. These preliminary results serve to validate a new postural control model, opening the door to the types of neural recordings and circuit manipulations that are currently possible only in mice.

Significance Statement

The ability to anticipate disturbances and adjust one's posture accordingly—known as "predictive postural control"—is crucial for preventing falls and for advancing robotics. Human postural studies often face limitations with measurement tools and sample sizes, hindering insight into underlying neural mechanisms. To address these limitations, we developed a postural perturbation task for freely moving mice, modeled after those used in human studies. Using a dynamic platform, we delivered reproducible perturbations with or without preceding auditory cues and quantified how the auditory cue affects postural responses to perturbations. Our work provides validation of a new postural control model, which opens the door to the types of neural population recordings and circuit manipulation that are currently possible only in mice.

Introduction

The ability to use prior information gained from experience in motor control is essential for all animals, enabling them to navigate and interact with complex and dynamic environments. It has been demonstrated that prediction plays a crucial role in our nervous system by serving as a basis for feedforward motor control and compensating for sensorimotor feedback delay and sensory noise(Dakin and Bolton, 2018; Wolpert and Flanagan, 2001), and such predictive control is integral to a wide spectrum of activities from fundamental movements to complex motor skills.

In addition to the execution of body movements, predictions also play an important role in efficient "postural control" – the process of maintaining upright posture and aligning body parts. Although it is often taken for granted, postural control is crucial in daily life, from maintaining equilibrium on an unstable surface (i.e. "balance") to stabilizing the body while executing movements. The issue of balance is of great clinical significance, given that falls constitute one of the leading causes of injury and death among the elderly population("CDC Older Adult Falls," 2023; Kannus et al., 2005) and neurological patients such as those with stroke(Denissen et al., 2019; Wei et al., 2019) or Parkinson's disease(Allen et al., 2022). While postural control has traditionally been thought of as a largely reflexive system mainly driven by sensory feedback, accumulating evidence shows that *prediction* plays an important role in postural control(Bastian, 2006; Dakin and Bolton, 2018; Jacobs and Horak, 2007). Sensory signals indicating an imminent loss of balance can trigger preparatory changes across the nervous system to mitigate the impending disruption to equilibrium.

In the present work, we focus on postural control to predictable external disturbances. This type of control can be illustrated by a simple example. Suppose you are riding in a train as part of your daily commute to work—a route you take every day. As you see that you are approaching the next station, based on the familiar scenery viewed through the window, you can expect that the train will decelerate, and you will consciously or subconsciously prepare even before the deceleration starts. In this case, your postural responses during deceleration might differ from occasions when the train slowed down unexpectedly.

Within the relevant literature, there are some differences among researchers regarding the definitions of different types of postural phenomena, necessitating a clarification of the terminology for the current study. Traditionally, responses to unpredictable, external postural perturbation to maintain equilibrium have been called **automatic postural responses** (**APR**)(Nashner and Cordo, 1981), or **compensatory postural adjustments** (or responses) (**CPA**)(Horak and Nashner, 1986). For simplicity, we will use CPA to refer to feedback control based solely on sensory afferents. Real-life examples of CPA in action would be the adjustments you rapidly make if you suddenly and unexpectedly get pushed from behind by another person, or, when riding in the subway, recover from a sudden acceleration or deceleration of the train. In addition to CPA, there is another kind of postural adjustment that *precedes and accompanies* voluntary movement to prepare and adjust the body for self-generated movement. These kinds of postural adjustments are called **anticipatory postural adjustments** (**APA**)(Massion, 1992). For example, if you are standing and trying to reach for a cup on the table in front of you, muscles in your legs will be activated even before the reaching arm starts moving. This activation of the leg muscles helps decrease the destabilizing effect of a shift in the body's center of mass produced by the extension of the arm. It is important to note that APA could occur *while* executing the movement, to maintain the equilibrium or stabilize body segments. This is also "anticipatory" in nature because the movements occur before there is any possibility of sensory feedback from the movement that can have an effect on response(Schepens and Drew, 2004). Some researchers use the words "preparatory APA" and "accompanying APA" to refer to APA that *precedes* and *occurs during* the movement, respectively(Schepens and Drew, 2004). Others include a postural adjustment that occurs before a predictable external perturbation as a type of APA(Santos et al., 2010). To avoid confusion, we suggest that the term APA should be applied only to the postural adjustments associated with voluntary movements(Massion, 1992). We will use the word "**predictive postural control**" to refer to postural adjustment or response to a predictable *external* perturbation. Predictive postural control includes 1) postural adjustments that *precede* the external perturbation(Jacobs et al., 2008; Mochizuki et al., 2008; Welch and Ting, 2014) such as leaning to one side, widening the stance and isometric contractions, and 2) (modulation of) postural responses that *occur during* the external perturbation (i.e., after the perturbation

onset) such as the scaling of gains(Lockhart and Ting, 2007; Pruszynski and Scott, 2012). We will use the term "feedback" to refer to corrective control mechanisms based on sensory afferents and the term "feedforward" to refer to control mechanisms that are set in advance and unchanged by online sensory feedback. Table 1 provides the categorization of postural adjustments that we will use, based on the timing and whether the postural disturbance is external or self-generated.

Human studies have contributed significantly to understanding predictive postural control, providing valuable insights into the modulation of postural responses by prediction and learning, but how exactly these mechanisms work in our nervous and biomechanical systems is mostly unexplained. In these studies, postural perturbations are usually presented to statically standing subjects by using a dynamic platform that produces a tilting or translational movement of a support surface in a controlled and reproducible manner. To study predictive postural control, scientists have used several different behavioral paradigms: 1) repetitive patterns of perturbations that rendered them predictable over time(Horak et al., 1989; Horak and Diener, 1994), 2) explicit visual/auditory cues that preceded perturbations and contained some information about the perturbation (e.g. timing and/or direction of the perturbation)(Coelho et al., 2017; Fujio et al., 2016; Jacobs et al., 2008; McChesney et al., 1996; Silva et al., 2015), or 3) classical conditioning paradigm where time-locked coupling of a tone (conditioned stimulus, CS) with a postural perturbation (unconditioned stimulus, US) were repetitively presented(Campbell et al., 2009; Kolb et al., 2004, 2002). Some brain regions such as the cerebellum and the cerebral cortex have been indicated for predictive postural control based on neurological patient studies(Horak and Diener, 1994; Kolb et al., 2004) and electroencephalography (EEG) studies(Jacobs et al., 2008; Mochizuki et al., 2008). However, the underlying neural mechanisms remain elusive as tools available for human studies are limited to coarse macroscopic measures, and human patient studies are often conducted on relatively small groups of patients with slightly different conditions, which hinders systematic evaluation.

Animal studies are necessary to take what we learned from these human studies to a more circuitry mechanism level of understanding, and our present approach with the mouse paradigm has several great advantages. Recently, a similar paradigm to human studies was established in bipedally standing rats in which rats experienced floor tilting perturbations that were always preceded by a visual stimulus of light with a fixed interval(Konosu et al., 2024, 2021). Researchers showed that the amplitude of the postural response diminished as the rats underwent more perturbations, which suggests plasticity in the postural control system of rats. This study also demonstrated that the human postural paradigm can be translated into rodent studies. Our current work goes further by explicitly testing the effect of prediction by comparing the postural responses to backward floor translations that were either unpredictable or

preceded by an auditory cue. We used mice over rats, because of the greater availability of genetically-modified animals such as transgenic mice expressing Cre or Flp recombinase. As a result, mice are more amenable to the following types of experiments than rats, let alone humans and non-human primates: 1. cell-type specific measurement and manipulation(Tsai et al., 2009; Zariwala et al., 2012; Zhang et al., 2010); 2. temporally specific neural manipulation (e.g. optogenetics and chemogenetics (Roth, 2016; Tsai et al., 2009; Zhang et al., 2010)); 3. circuit-specific neural labeling and manipulation using tracing technologies(Tervo et al., 2016; Wickersham et al., 2007). With these tools, the mouse model makes it possible to better define the neural structures involved and leads the way to more incisive experiments with humans, which would ultimately give rise to novel treatments that are eventually useful in clinical settings. Additionally, gaining insights into how our brains are wired to provide postural control may also contribute to advancements in robotics and control systems.

In the present work, we established a novel mouse paradigm to measure predictive postural control that is modeled after those used in human studies(Horak et al., 1989; Kolb et al., 2002; Welch and Ting, 2014) and recent rat studies(Konosu et al., 2024, 2021). In the following sections, we describe the postural task that we developed and how we quantified the postural responses based on kinematics and reward acquisition. Using these measures, we show some examples of analyzing the effects of a preceding cue and learning on the postural responses. This mouse model system opens the door to exploring the neural mechanisms underpinning predictive postural control.

Table 1: Different Types of Postural Responses (adjustments)

	prediction	When	
		before	during
External perturbation	−	n/a	compensatory postural adjustment (or automatic postural response)
	+	Predictive Postural Control pre-perturbation postural adjustment	(possibly) feedforward component + feedback component* (*could be altered with prediction such as adjustment of gain)
Self-generated movement	(+)	preparatory anticipatory postural adjustment	accompanying anticipatory postural adjustment + feedback component

There are multiple ways in which predictive mechanisms can work to affect postural control. One way is the generation of postural adjustments that *precede* an external perturbation(Jacobs et al., 2008; Mochizuki et al., 2008; Welch and Ting, 2014), such as leaning to one side, widening the stance, isometric contractions, etc. Another way is the modulation of the postural response *during* the perturbation. Two possible mechanisms (that are not mutually exclusive) can be considered to produce such modulations. One mechanism is the (feedforward) adjustment of sensorimotor feedback parameters such as the scaling of gains(Lockhart and Ting, 2007; Pruszynski and Scott, 2012). In other words, the control gain of the feedback system can be pre-set before a perturbation occurs. Another possible mechanism is that the feedforward movement command is prepared in advance and gets discharged during the perturbation. In other words, feedforward control can work in parallel with the feedback mechanisms; the idea that is comparable to "accompanying APA(Schepens and Drew, 2004)."

Methods

Animals

3 adult male mice were used. Experiments were performed on C57/BL6 mice, aged 10-26 weeks (two mice [mouse CB5 and CB6] were 13 weeks old at the start of pre-training, 24-26 weeks old during the full task experiments, one mouse [mouse CB10] was 10 weeks old at the start of pre-training, 14-16 weeks old during the full task experiments). Recordings were conducted between 9:00 and 18:00. Animals were individually housed throughout the experiments. All procedures were performed in accordance with the National Institutes of Health Guide for the Care and Use of Laboratory Animals and

approved by the Harvard Animal Care and Use Committee. This study was approved by the Ethical Committee for Animal Experiments at the University of Tokyo, and was carried out in accordance with the Guidelines for Research with Experimental Animals of the University of Tokyo. This study was carried out in compliance with the ARRIVE guidelines.

Predictive postural control task

We developed a postural perturbation task in freely moving mice, modeled after those used in human studies(Horak et al., 1989; Kolb et al., 2002; Welch and Ting, 2014) and a recent rat study(Konosu et al., 2021), in which a dynamic platform is used to give reproducible perturbations.

Water-restricted mice were placed in a clear acrylic box with a perch to stand on to access the lick spout for water reward (Figure 1a). The height of the lick spout was adjusted such that mice could just barely reach it by standing on their two hind legs (bipedal standing) while balancing on the perch. In other words, mice were required to stand on the perch to obtain water reward, which constrained the standing position and body orientation of the mice. A light-emitting diode (LED) indicated that mice were eligible to start a trial. Mice initiated the trial by licking the spout, which was monitored by a capacitive sensor.

In each trial, a reward water droplet (2 µl) was given immediately after the first lick. In order to keep the trial active, mice had to continue licking within an interval of 600 milliseconds (msec). Subsequent water droplets were given for each lick that occurred at least 1,100 msec after the previous reward. The height of the lick spout and the requirement of continuous licking, enforced by the maximum 600 msec window with no lick, encouraged the mice not to make large postural changes. The maximum duration of a trial was 7.5 seconds and mice could receive a maximum of 7 water droplets per trial. A trial was terminated in one of two ways: (1) If mice were able to continue licking the spout for the entire 7.5 seconds, the trial was deemed “complete”; (2) If mice failed to lick within any 600-msec interval, the trial was classified as “abort.” At the end of each trial, the LED was turned off and mice had to wait for an inter-trial duration of 10 - 15 sec (drawn from a uniform distribution) until the next trial could be initiated. For aborted trials, an additional 20 sec was added to the inter-trial duration as a penalty. In trials with a “perturbation,” mice experienced a backward movement of the entire behavior box, including the perch and the lick spout. A platform displacement occurred after a random delay from the first lick, which was drawn from a truncated exponential distribution (minimum, 2.5 sec; maximum, 6 sec; mean, 1 sec) to minimize the predictability of the timing. Note that if the trial was aborted before the cue or the perturbation, the same trial type was repeated for the next trial.

In order to test whether predictability affects postural responses, we used three different trial types (Figure 1b): (1) trials in which an auditory cue preceded platform movement by 1 second (CUE,

74% of trials); (2) trials in which the platform moved but no cue was given (NOCUE, 13%); and (3) trials with no platform movement (BLANK, 13%). For CUE trials, a 6 kHz tone began 1 sec before the onset of platform movement and terminated at the end of platform movement (Figure 1c). The reason for including BLANK trials is to generate uncertainty about whether the perturbation would happen or not, and to strengthen the relation of perturbation to the cue. All three trial types were randomly interleaved. In each daily session, mice performed 67-119 trials (median = 83 trials). The platform was moved in one of three amplitudes: 7 (small, only used for mouse CB10), 12 (medium), or 18 (large) millimeters. Only one amplitude was used for any single session.

For the sake of brevity, we will refer to perturbation trials (CUE trials and NOCUE trials), which constituted 87% of all trials, simply as “trials”, and we will specifically indicate “BLANK trials” when appropriate. BLANK trials are excluded from the following analyses. Note that trial indexing is based on all trial types (including BLANK trials).

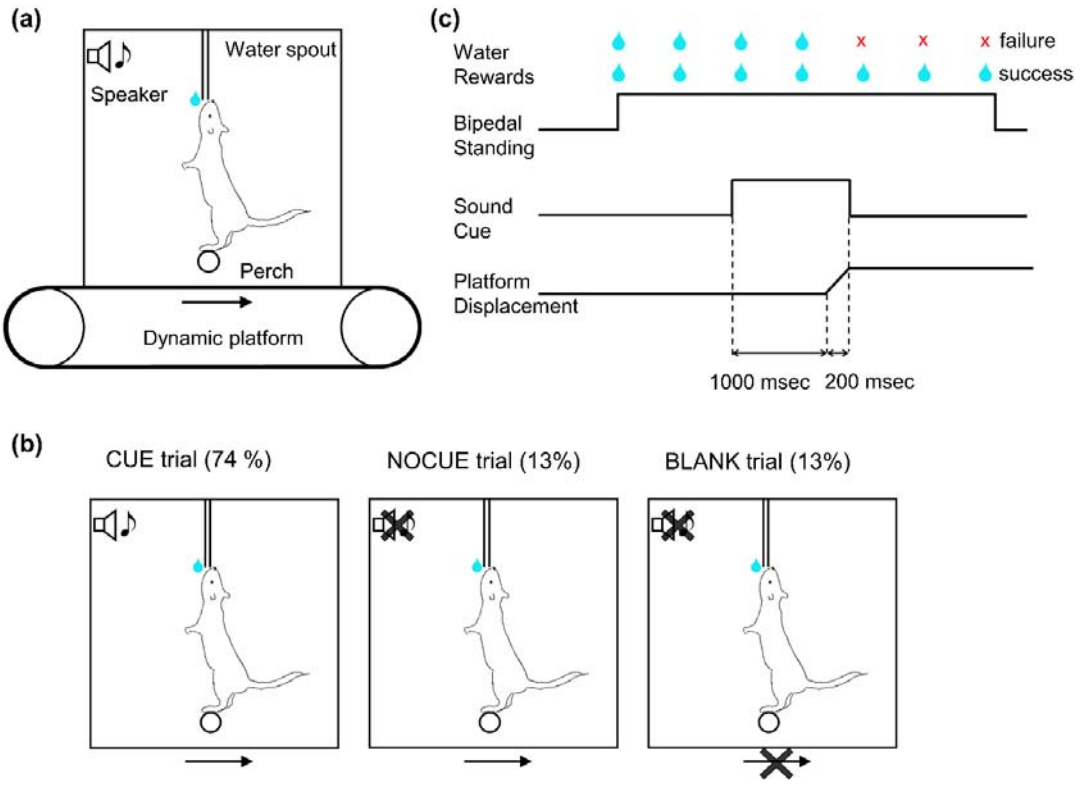

Figure 1: Postural task

(a) Diagram of behavioral apparatus. Mice stood on a round perch to receive water rewards from the lick spout. Both the perch and the water spout were fixed to the behavioral box. The behavioral box was mounted on a dynamic platform that created horizontal movement of the box.

(b) Diagram of three different trial types. (1) trials in which a cue preceded platform movement by 1 second. (CUE, 74% of trials); (2) trials in which the platform moved but no cue was given (NOCUE, 13%); and (3) trials with no platform movement (BLANK, 13%)

(c) Schematic depicting trial structure in the most common trial type (CUE trials). Mice initiated the trial by licking, which was immediately rewarded with a water droplet (2 µl). Postural perturbations consisted of a backward platform displacement lasting 200 msec. A sound cue was played preceding the perturbation by 1 sec and terminating at the end of the platform movement.

Behavioral apparatus

Custom hardware and software were used so that the task could run in a semi-automated way with pre-set task parameters using a closed-loop system (Figure 2). Since our paradigm uses an open-source programmable microcontroller that offers a flexible design of the task, it can easily be modified and applied to different postural tasks that ask different questions.

Hardware

A behavioral box was developed that allowed the recording of free movement (Figure 2a, see Table 2 for parts list). Mice were able to move freely in a 180 mm by 180 mm box. An acrylic rod of 10

mm diameter was fixed so that the top of the rod was 24 mm above the floor. Bright blue LED light illuminated the box from above to indicate the trial period. An audio speaker was mounted above the box to produce sound cues. A lick spout was hung from the ceiling of the box, and the height of the spout end was adjusted for individual mice. The lick spout was connected to a capacitive sensor that detected licks. The water pump was calibrated so that 2 μL of water was dispensed from the end of the spout for each water droplet delivery. To record the movement of the mice, four cameras were mounted around the box. The box was placed on a dynamic platform that can be moved in the horizontal direction in a timed manner. The task was controlled by Arduino UNO microcontrollers (Arduino, Somerville, MA), and task parameters and events were recorded to a computer via a data acquisition board (USB-6002; National Instruments, Austin, TX). Arduino UNOs were programmed to execute the task structure described in the task section and were wired to communicate with electronics such as the capacitive sensor, motor driver, speaker, water pump, and LED.

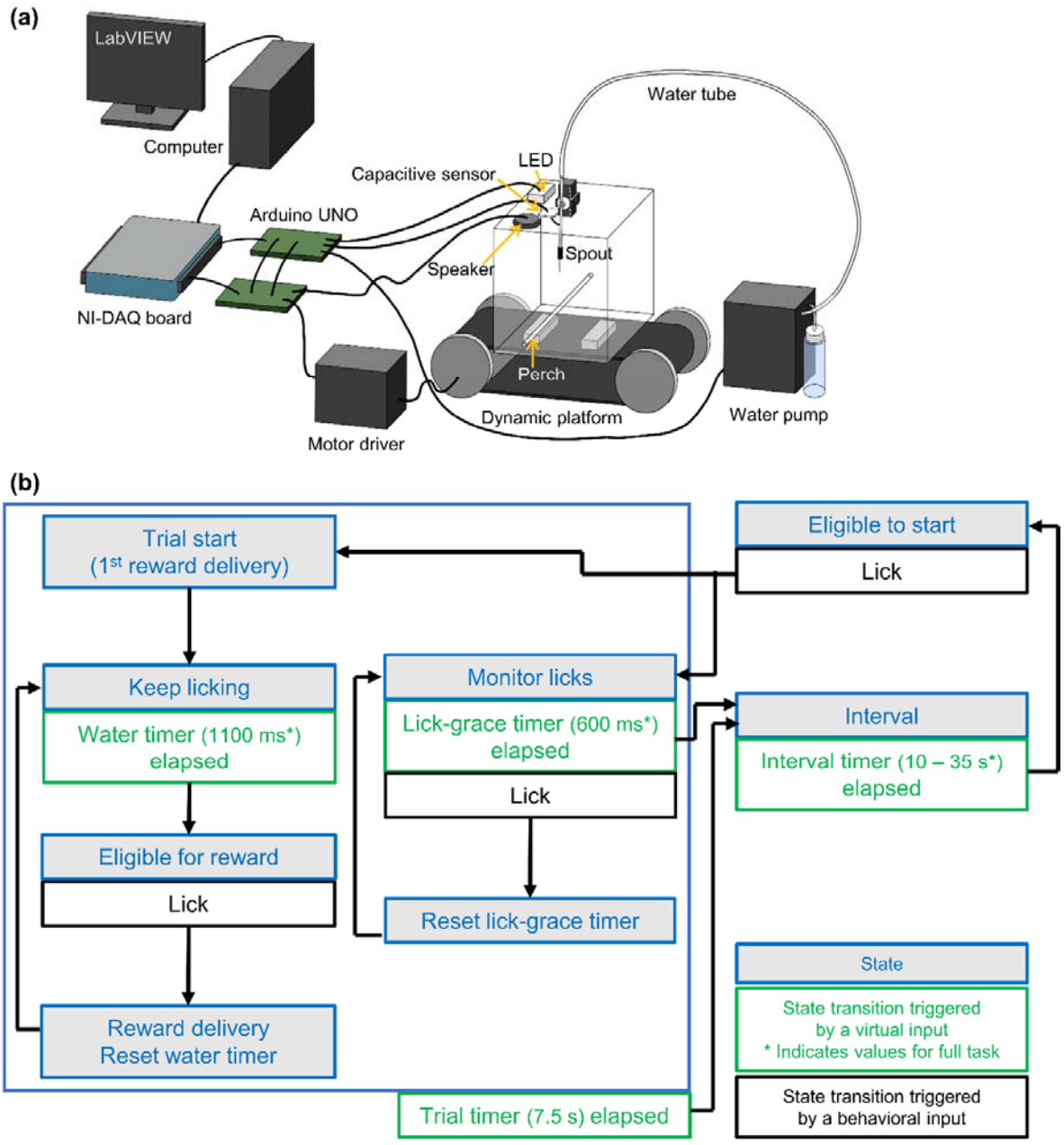

Figure 2: Experiment apparatus and task design

(a) Design of the experimental apparatus. A box made of clear acrylic was mounted on a dynamic platform. A round rod (perch), water spout, LED, and capacitive sensor were fixed to the box. Two microcontrollers (Arduino UNOs) were connected to the electronics to run the task in a closed-loop system. Video cameras and a synchronization device were omitted from the diagram for simplicity. See Table 2 for the parts list.

(b) Task state machine. States (blue) could transition either by a lick (behavioral input, black) or an elapsed timer (virtual input, green).

Table 2: Parts List

Part	Name/Description	Link
Walls/floor	Clear acrylic (thickness: 4mm)	https://www.hazaiya.co.jp/item/19037.html
Perch	Clear acrylic rod (diameter:10mm)	https://www.monotaro.com/g/02476005/
Lick spout	Stainless steel tube (20G)	https://www.nazme.co.jp/product/9-0-serviceinformation/9-5-information/kn-sus-p/
Touch sensor	Capacitive sensor	https://www.adafruit.com/product/1982
Speaker	Full range speaker	https://www.digikey.jp/ja/products/detail/bdnc-holding-limited/BGC-D40-22-4-002/9842990
Audio amplifier	Class D amplifier	https://www.adafruit.com/product/1752
Lighting	LED array (blue)	https://akizukidenshi.com/catalog/g/gI-12344/
Camera	NaturalPoint, Optitrack Prime X 13	https://optitrack.com/cameras/primex-13/
Synchronization device	NaturalPoint, eSync2	https://optitrack.com/accessories/sync-networking/esync-2/
Microcontroller	Arduino UNO	https://store.arduino.cc/products/arduino-uno-rev3
Data acquisition system	National Instruments, USB-6002	https://www.ni.com/en-us/support/model.usb-6002.html

Task implementation

There were two phases in the behavioral paradigm: pre-training and full task. During pre-training, mice learned the trial-interval structure with progressive parameters over sessions. In the full task, mice experienced sound cues and platform motion (hereafter referred to as a "perturbation"), and it was during this phase that we investigated the animals' postural responses.

Pre-training

Before testing mice on the full version of the task in which they experienced perturbations, they were trained on a simpler task. The goal of this pre-training was to train mice to stand bipedally during the trial period and not to stand during the interval period. This trial-interval structure was important for two main reasons: 1) to control the timing of the perturbation relative to the onset of standing so that mice were not standing for a too short or too long period of time before the perturbation, and 2) to motivate

mice to perform well by limiting the time when they could obtain water rewards. With the trial-interval structure, if mice failed to perform well in a trial and did not get as many water droplets, they had to wait for the duration of the interval period until the next trial became available to start.

The trial-interval structure was as follows (also see Figure 2b):

A blue LED light turned on to indicate that the mouse was eligible to start a trial. As soon as a lick was registered while the LED was on, the trial started, and the first water droplet was given.

In order to keep the trial active, the mouse had to lick at least once within a 600 msec interval (referred to as "lick-grace timer" in Figure 2b). After each lick, the 600-msec lick-timer was re-started, so that any lick-free period of >600 msec resulted in termination of the trial (see below). However, not every lick was rewarded—a water droplet was only given for licks that occurred at least 1100 msec *after* the previous reward (referred to as "water timer" in Figure 2b). Thus, the maximum number of rewards the mouse could receive on a single trial was 7 drops, but the mouse needs to lick more frequently than this to keep the trial active. An example sequence of licks and rewards in the full task is shown in Figure 3d and 3h.

A trial could terminate in one of two ways: 1) a 'complete' trial if the mouse continued licking throughout the full 7.5 seconds; 2) an 'aborted' trial if the mouse failed to lick for 600 msec. When the trial was terminated either way, the LED was turned off and the inter-trial interval started.

During the inter-trial interval, the spout did not dispense water even if licking was detected. On each trial, the duration of the inter-trial interval was drawn from a uniform distribution of 10-15 seconds. For aborted trials, 20 seconds was added to the interval duration (additional penalty interval). This lengthy "time out" for aborted trials was enforced to encourage the mouse to get as much water as possible on each trial, rather than to bail early and move on to the next trial. Before a new trial could be started, the mouse had to refrain from licking for 5 seconds. This "no lick" period was included so that the mouse did not lick continuously throughout the inter-trial interval. Additionally, a trial was manually aborted by the experimenter if the mouse faced the wrong direction to make the posture of the mouse more consistent across trials. This manual intervention was effective and standing in the opposite direction rarely occurred during the final few sessions of the pre-training and the full task sessions.

Over the multiple sessions of pre-training, task parameters, such as the water timer, were gradually modified to reach their final values that are shown in Figure 2b. After mice experienced the pre-training with final task parameters for 5-6 sessions, they started the full task.

Full task

On top of the trial interval structure that mice learned during pre-training, the sound cue and platform movement were added to the task. The structure of the full task was explained in the subsection "Novel postural task for mice" in the Methods section.

Perturbation profiles

Though the effect of different perturbation amplitudes was not systematically studied, we explored a few different ones in our pilot experiments to see what was reasonable for the mouse. In what follows, we chose a perturbation size of 18 mm (large) as one that was big enough to be challenging for the mice but not so large as to be impossible to compensate. We also used the perturbation sizes of 7 mm (small, only used for mouse CB10) and 12 mm (medium) as milder ones. For the three platform displacement amplitudes, peak velocity was 60 mm/sec (small, only used for mouse CB10), 100 mm/sec (medium), and 140 mm/sec (large) respectively. Only one amplitude was used for any single session.

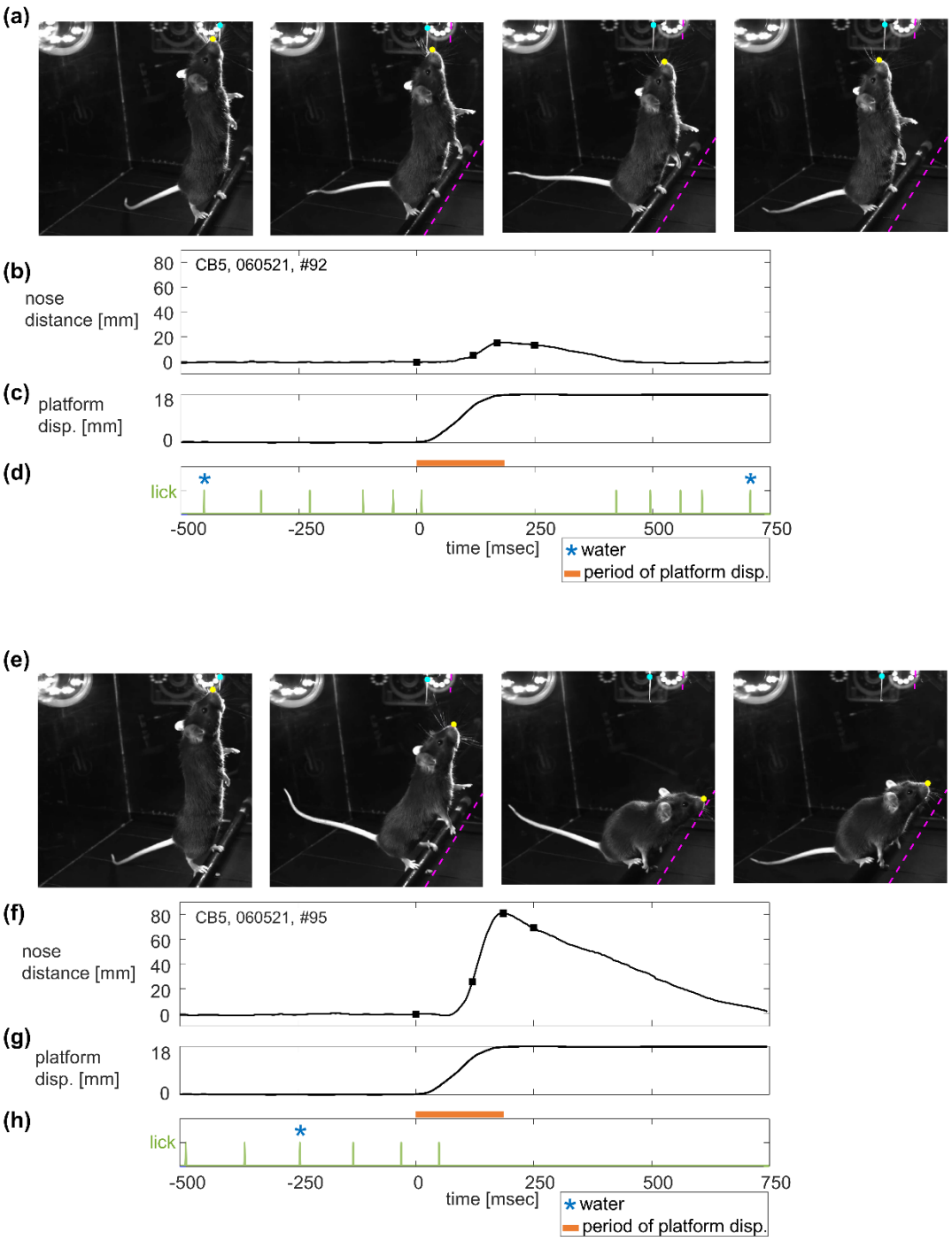

Figure 3 : Postural responses to the backward perturbation

This figure shows data from an example mouse (mouse CB5).

(a) Representative snapshots from a recorded video of a successful trial: 1. perturbation onset, 2. 125 msec after perturbation onset, 3. time of maximum nose distance, 4. 250 msec after perturbation onset. Cyan and yellow circles indicate the spout and nose positions that DeepLabCut tracked. Dashed magenta lines indicate the initial positions of the spout and the perch.

(b)-(d) Nose distance trace over time from the same trial along with the platform displacement and lick (green) and water (blue) events. Square dots indicating the timings of the snapshots are superimposed on the nose distance trace.

(e)-(h) Representative snapshots and time courses from a failed trial, depicted in the same way as (a)-(d).

Data Acquisition

Video recording

Four video cameras (OptiTrack; NaturalPoint, Corvallis, OR; Table 2) were mounted to surround the behavioral arena. Mice were videotaped at 200 fps with 1280 x 1024 pixels resolution, and data was saved using OptiTrack recording software, Motive (NaturalPoint). For the present analysis, we used only the data obtained by a single camera.

Event recording

The timing of critical trial events, such as LED onset, licks, rewards, and video frames, were marked by digital voltage signals (transistor–transistor logic or TTL) and recorded to the PC via a data acquisition board (USB-6002, National Instruments) controlled by custom scripts written with LabVIEW software (National Instruments). To synchronize the video data with trial events, an eSync 2 device (NaturalPoint) generated a voltage signal at the start of each video frame, and these signals were also recorded by the PC via the data acquisition board.

Data Processing and Analysis

Video tracking using DeepLabCut

A deep learning-based pose estimation system, DeepLabCut (Lauer et al., 2022; Mathis et al., 2018; Nath et al., 2019) version 2.3, was used to track key points of the mouse and the apparatus. From the perspective of motor control, one can hypothesize that the goal of the mouse is to control the location of their tongue close to the end of the lick spout. Thus, one good measure of postural response would be the distance of the control point (tongue) from the target (end of lick spout). Since the tongue was not constantly visible in the videos, we tracked the position of the nose. For the same reason, a visibly distinct part of the spout was tracked instead of the end of the lick spout (e.g., Figure 3a and 3e). Distance between these two tracked points (hereafter, “nose distance”) was used as an index of postural response.

After running DeepLabCut on each video file, the output files (CSV file with x/y coordinates of selected features and their corresponding likelihood values) were processed. The nose distance was obtained as the Euclidian distance between the nose and the spout in each video frame. The baseline nose distance was defined by taking the mean of the nose distance of 250 - 2250 msec before the perturbation onset and was used for subtraction. All nose distance values exceeding 450 pixels (= 81 mm) were maxed out to 450 pixels. At this distance, the mice came down from bipedal standing and their front paws were near the height of the perch. Nose distance values larger than this were often contaminated by the motions

of the animals that were not the target of interest (e.g., they stepped down from the perch or stepped to the right or left on the perch).

We removed certain trials from the analysis where the nose distance at the perturbation onset was more than 225 pixels (= 40.5 mm) (0.54% of all analyzed trials). A nose distance of 225 pixels or more at the perturbation onset indicates that the mouse was ducking down at the onset of the perturbation. This itself is an interesting behavior as it could indicate that mice are predicting the timing of the perturbation. However, if the initial posture was not standing upright, it did not make sense to compare responses to the perturbation. Therefore, those trials were excluded from the analysis.

We also note that 8 trials (0.36% of all analyzed trials) had to be excluded from the maximum nose distance analysis (explained in the following subsection) because no videos were recorded due to camera failures. The trial events data for these trials were intact and used for the trial outcome analysis.

Quantification of postural responses

Maximum nose distance

To quantify the postural performance for each trial, we used maximum distance of the nose position from the lick spout during the time window from the onset of the perturbation to 250 msec after the perturbation onset. We looked at other measures such as mean, median, and area under the trace, and found that the main results did not change.

Trial outcome

From the reward learning perspective, one can hypothesize that the goal of the mouse is to maximize the amount of water reward that they obtain on a given trial. Thus, we defined another performance index based on rewards that the mouse obtained. In a given trial, if mice obtained at least one water droplet after the perturbation, we classified the trial as a "success." In a given trial, if mice obtained no water droplet after the perturbation, we classified it as a "failure". We call whether a trial was a success or failure the "trial outcome." Note that if mice failed to lick within the 600-msec interval, the trial was aborted (see Methods; Predictive postural control task). Therefore, if mice could not recover to the lick spout quickly enough and lick again after the perturbation, they could no longer obtain any water reward (see Figure 3 for a graphical explanation).

In a successful trial, mice tended to get the maximum number of water droplets (7 droplets per trial) unless they stopped licking during the post-perturbation period (Figure 4). In a failed trial, mice received a few water droplets before perturbation and no reward after the perturbation (Figure 4). Consequently, the total number of water droplets mice received in a failed trial varied depending on the timing of the perturbation.

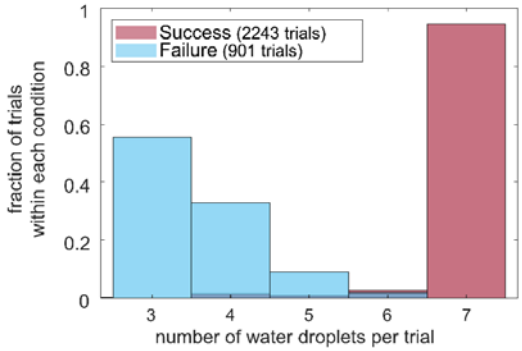

Figure 4: Distribution of number of received water droplets per trial.

Distribution of the number of received water droplets per trial for success and failure from all three animals.

Regression models

We used regression models to analyze the effect of the sound cue and learning on the postural responses.

Exponential decay model to predict the maximum nose distance

For each animal, we performed nonlinear regression (using the 'fitnlm' function in MATLAB; MathWorks, Natick, MA) to individual trial data, to predict the maximum nose distance based on two input variables - namely, whether a trial was cued or not (indicator variable) and the session index (order of experimental sessions across days). We used an exponential decay model as it is one of the most traditional models of learning and is also used in human postural perturbation studies(Kolb et al., 2004, 2002, 2000) (series of work from Kolb et al.). We did not incorporate the trial index as a variable in this model because we did not see a consistent trend based on it across sessions. We will discuss the effect of it in a separate section.

Equation 1 describes standard decay function:

$$D = A * exp\left(-\frac{session}{\tau}\right) + C \quad \ldots \quad (1)$$

, where D corresponds to the maximum nose distance and "*session*" corresponds to the session index. A, τ, and C are the coefficients to be fit by the regression, where A represents the amplitudes of the decay component, τ is the decay time constant across sessions, and C is an offset.

To incorporate the effect of the cue, we used the "learning rate model," in which the cue affects the learning rate (time constant, τ, in Equation 1). The learning rate model would indicate that the cue somehow speeds up or slows down the associative process of learning over sessions.

This model can be formulated in the following equation.

$$D = A * exp\left(-\frac{session}{\tau + \tau_c \cdot cue}\right) + C \quad \ldots \quad (2)$$

In this equation, "*cue*" is equal to 0 on NOCUE trials and 1 on CUE trials. A, τ, τ_c, and C are the coefficients to be fit by the regression; τ_c represents the effect of the cue on the time constant. A negative value for τ_c would mean that mice learn faster over cued trials, and vice versa.

Logistic regression model to predict the trial outcome

For each animal, we performed logistic regression (using the generalized linear model; 'fitglm' in MATLAB) to individual trial data, to predict the trial outcome based on whether a trial was cued or not (indicator variable), the session index, and the trial index. Equation 3 describes this relationship:

$$log\left(\frac{P}{1-P}\right) = \beta_0 + (\beta_1 \cdot cue) + (\beta_2 \cdot trial) + (\beta_3 \cdot sesion) \quad \ldots (3)$$

or equivalently,

$$P = \frac{1}{1 + exp\left[-\left(\beta_0 + (\beta_1 \cdot cue) + (\beta_2 \cdot trial) + (\beta_3 \cdot sesion)\right)\right]}$$

, where "P" corresponds to the probability of success and β_0, β_1, β_2, and β_3 are the coefficients to be fit by the regression. β_0 is a coefficient that represents the log-odds of a successful trial without any prior experience of the task or the cue. β_1 is a coefficient representing the effect of cue on the trial outcome. β_1 is multiplied by "*cue*," which is equal to 0 on NOCUE trials and 1 on CUE trials. β_2 models the effect of trial index on the trial outcome; "*trial*" is the trial index within a session. β_3 is the coefficient corresponding to the effect of session index on the trial outcome.

Statistical analysis

Data analysis was performed using custom scripts written in MATLAB R2020a (MathWorks). For each animal, one regression model and one logistic regression model were fit using MATLAB's fitnlm() function and fitglm() function, respectively: one to predict nose distance and one to predict the outcome of the trial.

Results

The movements of the mice were simultaneously recorded by four cameras which were mounted to surround the behavioral arena (Figure 5). In the present work, we analyzed the videos from one camera as data from a single camera was sufficient to demonstrate the validity of the task. The behavioral and task events such as licking, cue onset, and water deliveries were also recorded and synchronized with the video recordings, and this allowed event-based analyses (Figure 2; see Methods for the details).

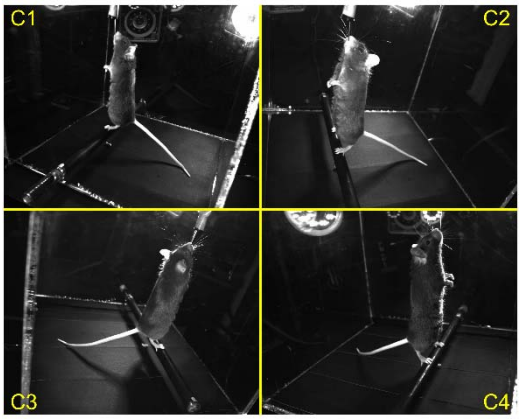

Figure 5: Views from four cameras
An example simultaneous view from four cameras during the task. The analysis in this paper is using C4 camera only.

Here, we will show two quantifications; one using the tracked video data and the other using recorded behavioral and task events, as an example of what one can readily measure using our task. Then, we will demonstrate the measurable effect of cue and learning using these two quantifications. In order to quantify the postural performance for each trial, we used two indices: (1) maximum distance of the nose position from the lick spout during the time window from the onset of the perturbation to 250 msec after perturbation onset (the maximum nose distance) (Figure 6a magenta lines showing the time window), and (2) whether the animal obtained at least one water reward after the end of perturbation (trial outcome).

For illustration purposes, four representative snapshots from a recorded video of a successful trial and a failed trial from one of the cameras are shown in Figure 3a and 3e respectively: Frame 1, perturbation onset; Frame 2, 125 msec after perturbation onset (the middle time point of the time window for calculating maximum nose distance); Frame 3, time of maximum nose distance; Frame 4, 250 msec after perturbation onset (the end of the time window for calculating maximum nose distance). In most of the trials, the backward platform movement produced forward movement of the mouse's body, which is consistent with the human postural responses to backward perturbations(Horak and Nashner, 1986). Typically, the tail tip and the heels went up with forward movement of the whole body and then went back down as mice recovered to the upright position. See Video 1 (successful trial) and Video 2 (failed trial) for the same representative trials (at 0.25x speed).

Nose distance

The time series of nose distance of the same representative trials are shown in Figure 3b and 3f with square dots indicating the timing of snapshots along with the time course of platform displacement (Figure 3c and 3g). From these representative traces, we can see that there was about 50 – 100 msec of delay between the onset of the perturbation and the onset of the nose distance displacement. This kind of delay is consistent with what was observed in the human postural paradigm(Welch and Ting, 2014). The representative traces also showed that the nose distance peaked near the end of the perturbation and gradually recovered to the baseline as mice reassumed an upright posture. The descending recovery slopes were more gradual than the ascending slopes. We also note that, although not depicted in these example trial traces, there were cases where we observed changes in nose distance and other kinematics before the perturbation onset. This could be a sign of anticipation or learning and could also modulate the postural responses to the perturbation.

Figure 6 shows the nose distance data from this mouse. The mouse experienced medium-amplitude perturbations on session #1 through #5, and large-amplitude perturbations on session #6 through #16 (Figure 6a). In Figure 6b, multiple nose distance traces for the first (left) and last (right) sessions of the large perturbation days are shown. The traces are aligned to the perturbation onset, and every 3rd trial is plotted for visualization purposes. We observed some variability in the onset of nose displacement and the timing of the peak, but the overall time course is consistent: peaking near the end of the perturbation and more gradual recovery.

The maximum nose distance fluctuated across trials (Figure 6b, c). However, on average, the last session had smaller maximum nose distances compared to the first session of the large perturbation days. In one of the example sessions shown in Figure 6c, the maximum nose distance was relatively large at the

beginning of the session but was reduced throughout the rest of the session (session #16, the last day of large perturbation). On the other hand, in the other session shown in Figure 6c, a trend across trials was barely apparent (session #6, the first day of large perturbation). The overall postural performance for each session was summarized by the mean and standard error of maximum nose distances (Figure 6d for mouse CB5).

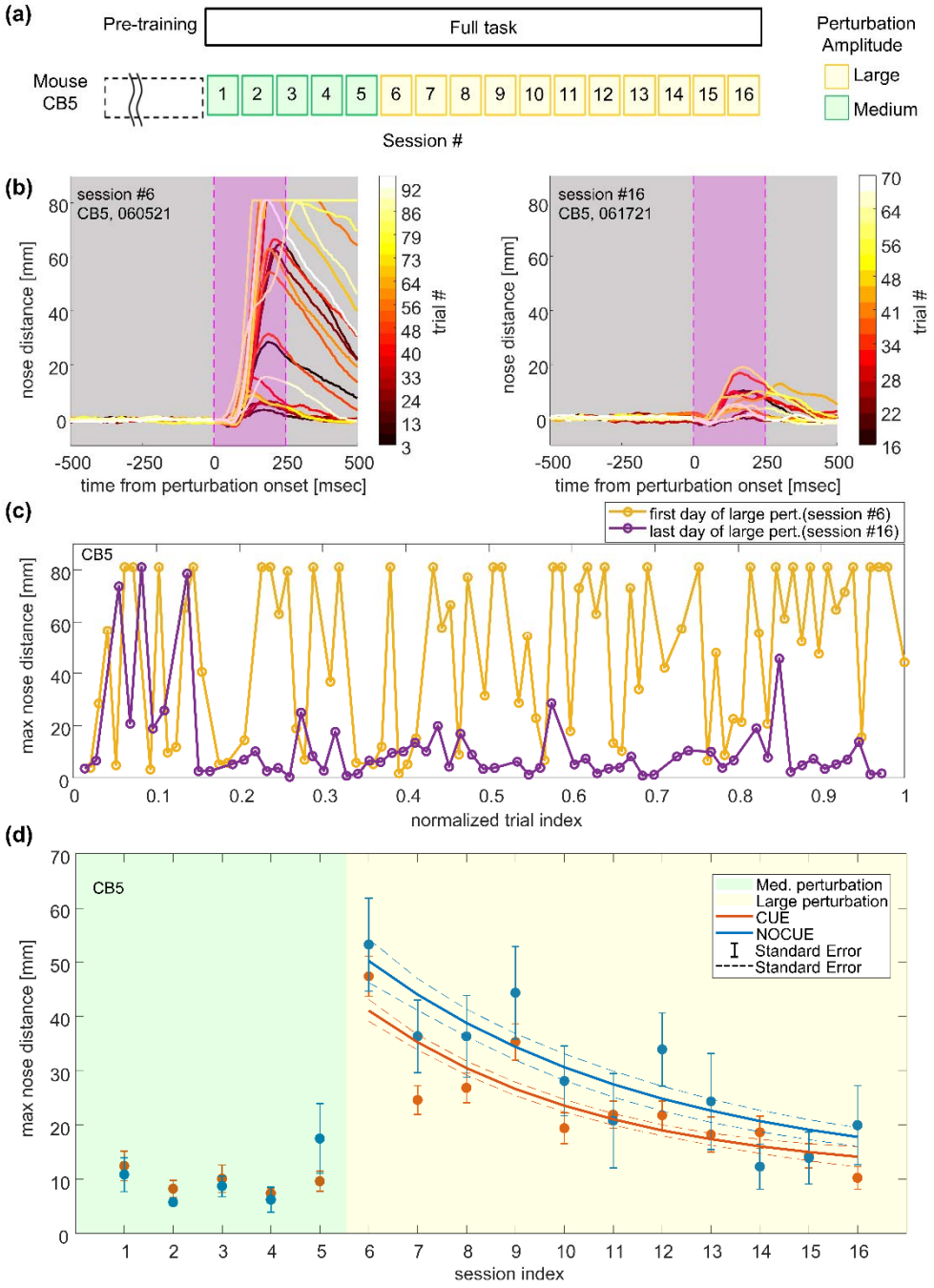

Figure 6 : Data analysis based on nose distance

This figure shows data from an example mouse (mouse CB5).

(a) Time course of sessions. The platform was moved in one of three amplitudes: 7 (small), 12 (medium), or 18 (large) mm. Only one amplitude was used for an individual session.

(b) Nose distance traces for the first session (left) and last session (right) of large (18 mm) disturbance days. Every 3 trials are plotted, and traces are color-coded by trial index. Note that trials 1-12 of the last session were excluded from this figure due to the low quality of DeepLabCut tracking. However, the max nose distances of those trials were manually extracted using ImageJ and used in the following figures and analysis (see Methods).

(c) Max nose distances across all trials for the first session (yellow) and last session (purple) of large disturbance days. Trial indexes are normalized by the total number of trials (82 and 63 trials for the first and last session respectively) of the session.
(d) Mean and standard errors of the max nose distance across all the sessions. Lines show fit from an exponential decay model ("learning rate model"). Dashed lines represent standard errors for fits.

Trial outcome

The timing of licks and water deliveries of the same representative trials are shown in Figure 3d and 3h (mouse CB5). The mouse licked relatively constantly during the pre-perturbation period, and then could not lick for a certain amount of time due to the effect of postural perturbation.

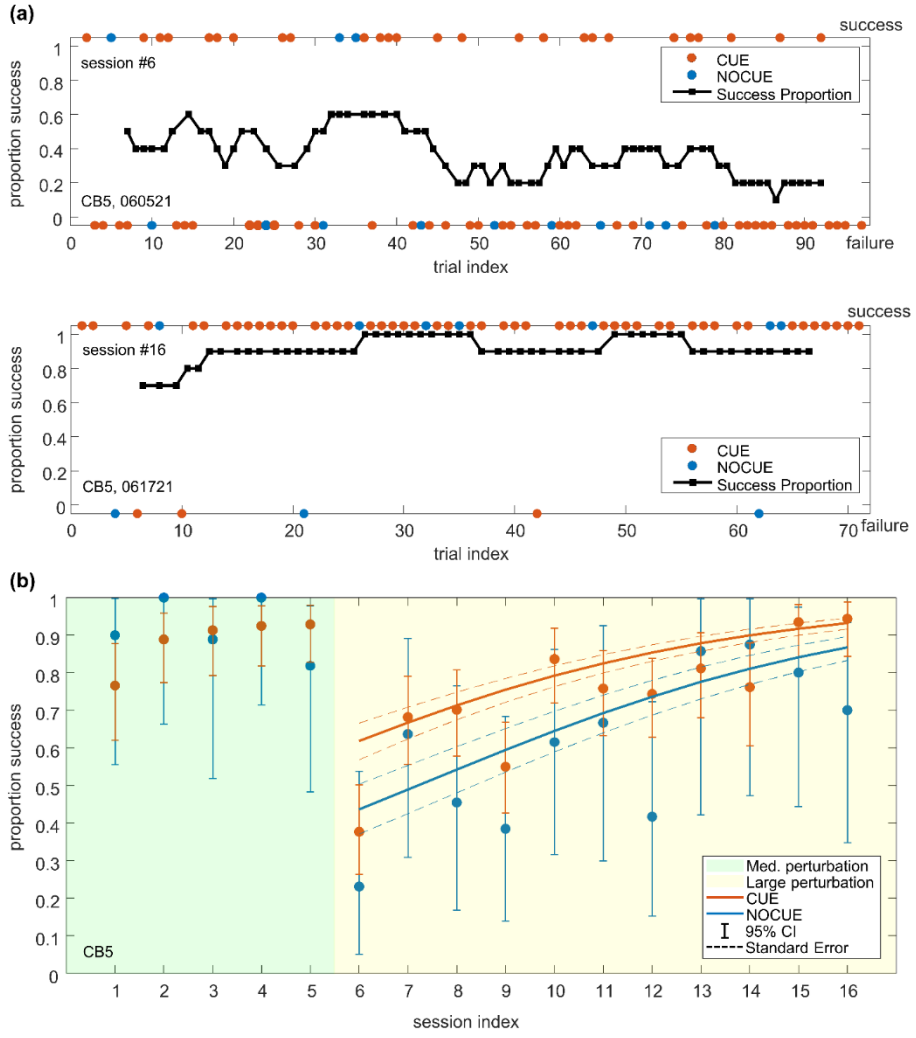

514 **Figure 7** shows the trial outcome data from this mouse (mouse CB5). The sliding window
515 proportion of success and every trial outcome in the first and last session of the large perturbation

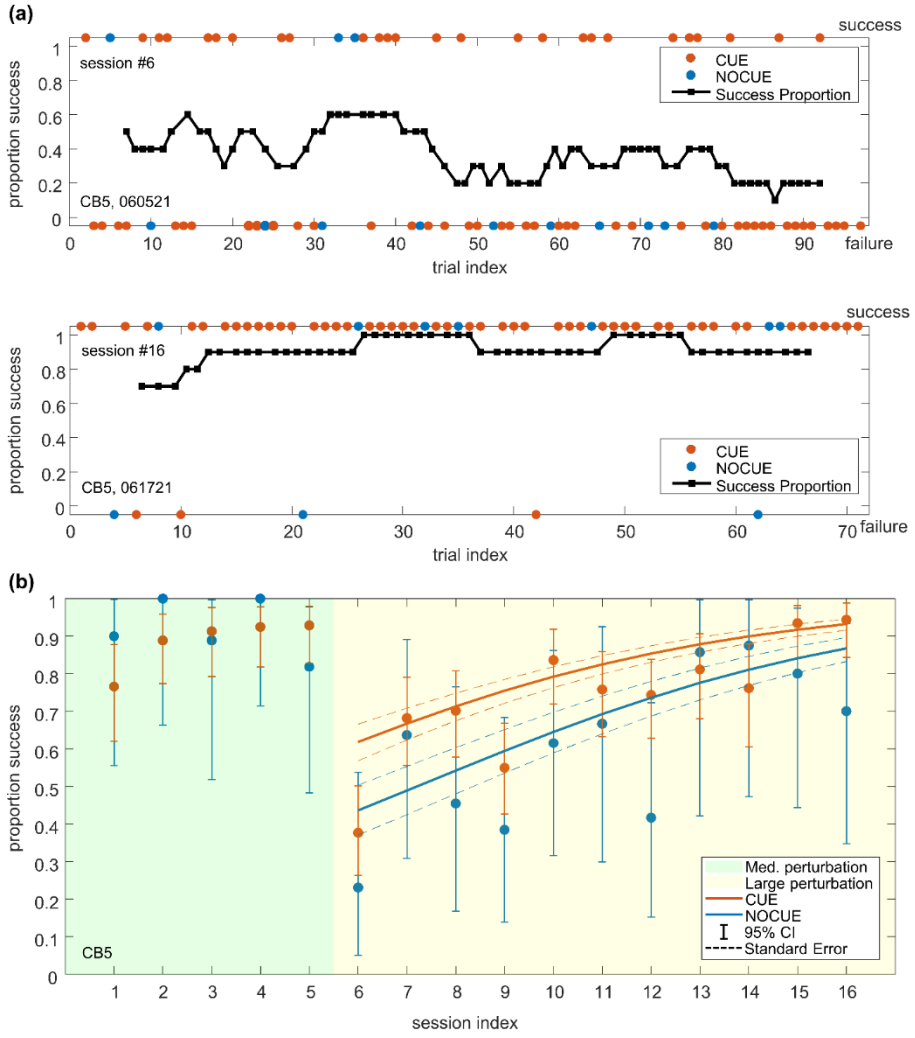

516 sessions are shown in

517

518 **Figure 7**a top and bottom respectively. Overall, the last session had a higher success proportion
519 than the first session. The overall postural performance of each session was summarized by the proportion

of successful trials over all the trials

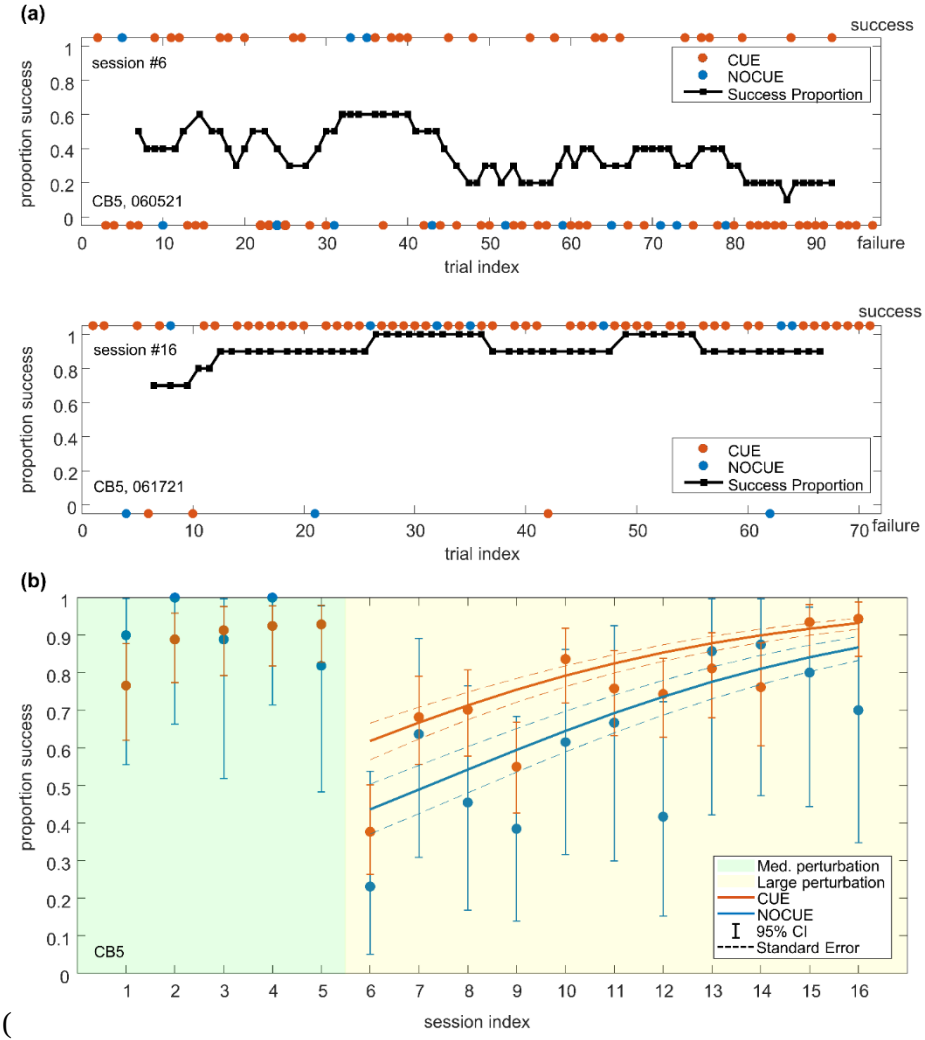

(

Figure 7b), and error bars represent 95% confidence intervals estimated based on the binomial distribution.

Measurable effect of cue and learning

To analyze the effect of the sound cue and learning on the postural responses, we used regression models (see Methods). These models allowed us to assess the strength of the relationship between postural responses and several predictor variables. This allowed us to simultaneously test whether animals' performance improved both within and between sessions and to determine whether the presence of a predictive cue affected performance while controlling for the other variables.

For this example mouse (mouse CB5), the exponential function (the predictor variables were: whether a trial was cued or not [indicator variable] and the session index; see Methods for details) described the trend over sessions in the maximum nose distance relatively well (adjusted R^2 = 0.13; Figure 6d, n = 795 trials, showing the fitted lines for the learning rate model; see Methods for the details of the model). This suggests that learning across sessions can be well characterized by an exponential decay function for maximum nose distance in this mouse. The model had a negative value for the cue-related coefficient (τ_c = −1.21, p = 0.058 in the learning rate model), which suggests that the cue works in the direction of *improving* the postural response. Table 3 shows the coefficients and p-values of the model for this mouse.

For the same mouse (CB5), we also examined the effect of within-session and across-session learning, and the effect of cue on the trial outcome using logistic regression (the predictor variables were: whether a trial was cued or not [indicator variable] and the session index, and the trial index within a session; see Methods for details), and found that the cue and the session index had significant positive regression coefficients ($e^{\beta 1}$ = 2.10, p = 0.00073; $e^{\beta 3}$ = 1.24, p <0.0001; Table 4) and the trial index had a negative regression coefficient ($e^{\beta 2}$ = 0.99, p = 0.033; Table 4). Exponentiated coefficients represent the effect size of the cue in terms of the odds-ratio in logistic regression. Thus, these results indicate that the odds of a successful trial are 2.10-fold higher with the cue compared to without the cue and that one increment in the session index multiplies the odds of a successful trial by 1.24 and one increment in the

550 trial index multiplies the odds of a successful trial by 0.99 for this mouse (

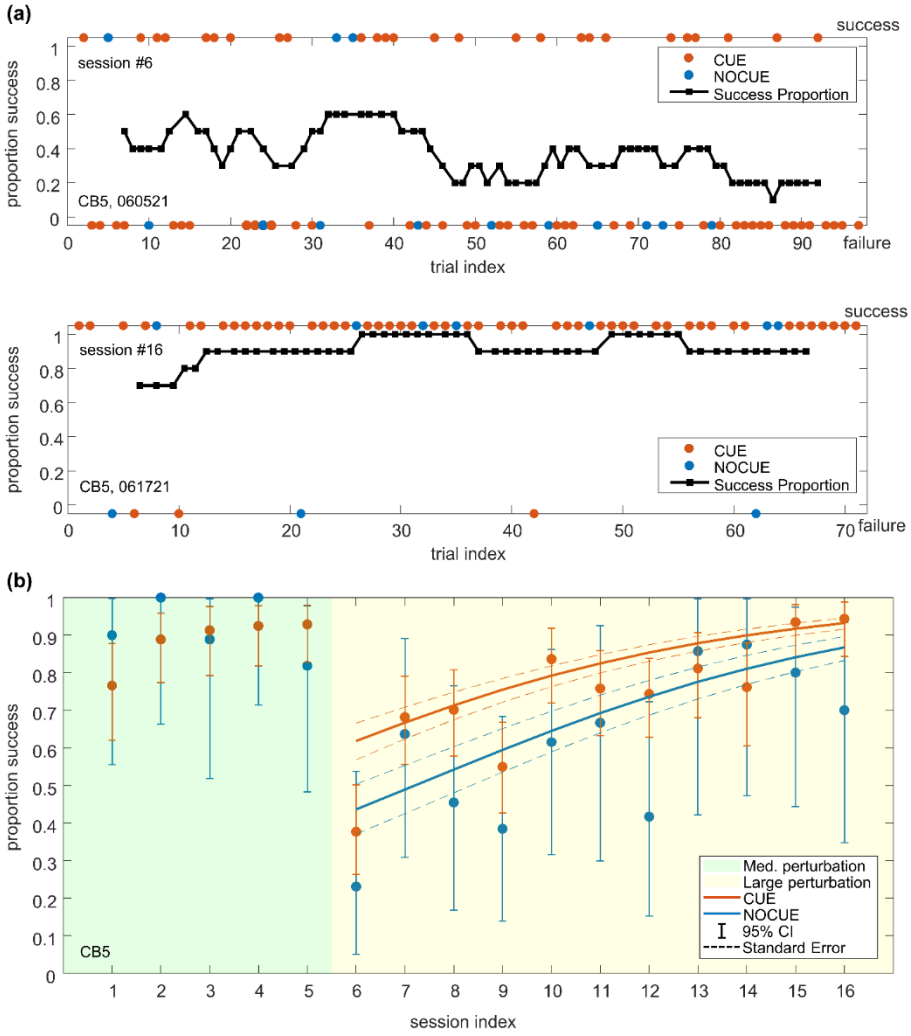

551

552

553 **Figure 7**b, *n* = 797 trials; see also Table 4).

554

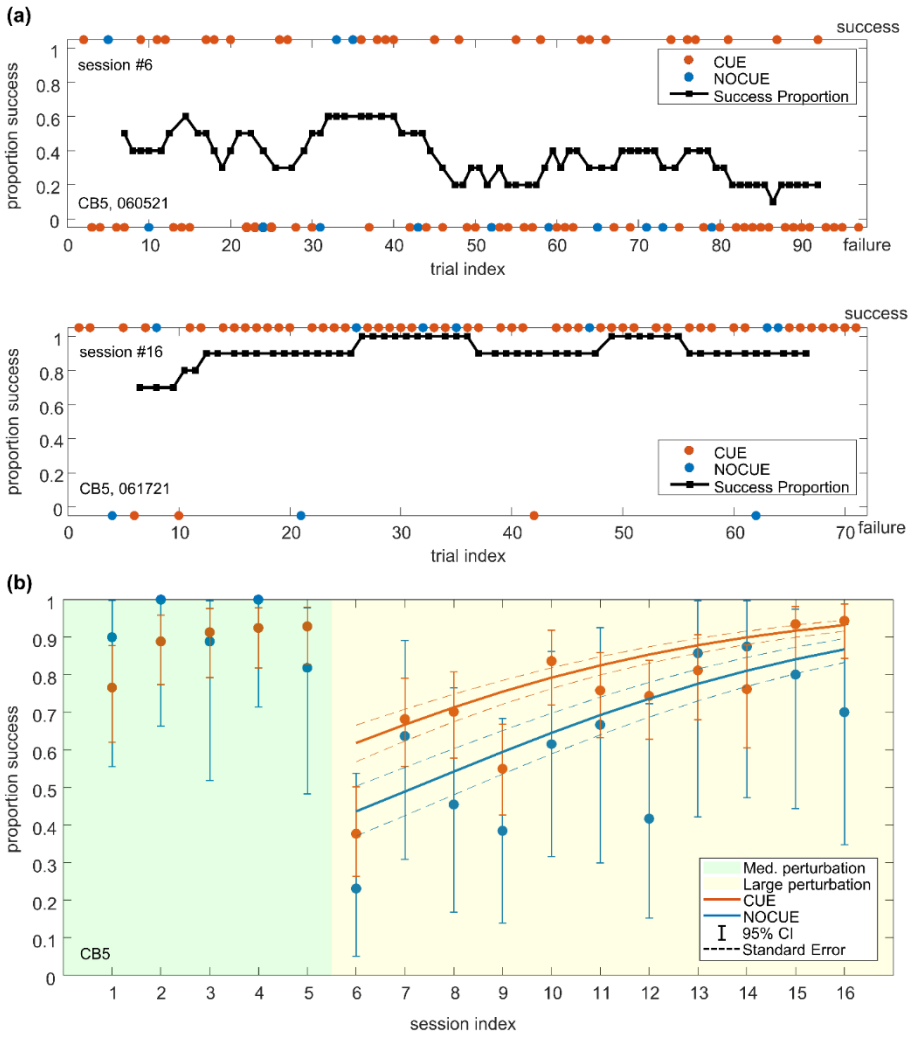

Figure 7: Data analysis based on success proportion

This figure shows data from an example mouse (mouse CB5).

(a) The sliding window proportion of successes (sliding window size = 10, black) and every trial outcome (colored circles) in the first (top) and last (bottom) session of the large perturbation sessions.

(b) The success proportion with 95% confidence intervals across all sessions. Solid lines show fits from logistic regression for CUE and NOCUE conditions. Dashed lines represent standard errors for fits.

Table 3: Exponential Decay Regression Models Coefficients and Statistics

Mouse CB5 (learning rate model, AIC =7270.6)

	Coefficients	**Standard Errors**	**P-Values**
A	110	35	0.0016*
τ	5.9	2.0	0.0036*
τ_c	-1.2	0.6	0.058
C	10.5	4.6	0.023*

* indicates significant value ($p < 0.05$)

Table 4: Logistic Regression Model Coefficients and Statistics

Mouse CB5

	Exponentiated Coefficients	**Exponentiated Standard Errors**	**P-Values**
β_0	0.22	1.48	0.00010*
β_1 (cue)	2.10	1.24	0.00073*
β_2 (trial)	0.99	1.00	0.0033*
β_3 (session)	1.24	1.03	$<$ 0.0001*

* indicates significant value ($p < 0.05$)

Discussion

In this study, we established a novel postural task for mice that enables studies of predictive postural control circuits. We validated the task by investigating the effects of a preceding cue and learning on postural responses. In our task, mice experienced external balance perturbations that were either

595 preceded by a time-locked auditory cue or were unpredictable. Using a small sample of animals, we
596 demonstrated that a combination of video recordings and event data can be used to study postural
597 responses to perturbations between predictable and unpredictable conditions, as well as over multiple
598 sessions.

599 This study sought to develop a postural experimental paradigm using mice, a species that is more
600 amenable to genetic and molecular tools that enable cell-type specific neural recording and manipulations,
601 to further mechanistic studies at the cellular and circuit levels, which is currently difficult in humans or
602 even in rats. Our approach used an open-source programmable microcontroller, such as Arduino UNO,
603 renowned for its versatile input/output capabilities and adaptable task design. This framework facilitates
604 smooth integration with various neural manipulation and recording devices and techniques. Furthermore,
605 its inherent flexibility allows for straightforward modification and application across diverse postural
606 tasks, enabling approaches to a range of research questions.

607 There are a few limitations and potential improvements in our study. First, we faced limitations in
608 the number of trials that mice performed during a single session, due to the nature of reward-based tasks
609 for mice. In particular, the number of NOCUE trials in a session was relatively limited, making it difficult
610 to compare the effect of learning within sessions between CUE and NOCUE conditions. Increasing the
611 proportion of NOCUE trials might be necessary to have more statistical power for analysis within
612 sessions. Yet, we note that the proportion of NOCUE trials should be low enough so that these NOCUE
613 trials are “surprising” to the mice. Second, we found that the time to initiate a trial was longer in later
614 trials (Figure 8), which might indicate that the animals were less engaged near the end of the session. This
615 is a common issue among behavioral experiments, especially the ones that utilize restrictions on water or
616 food consumption to create motivational drive(Berridge, 2004; Ortiz et al., 2020). It can pose a challenge
617 as the level of engagement can potentially confound task performance, in our case, the postural responses.
618 In future experiments, this might be mitigated by monitoring the time to initiate a trial online as an index
619 of the task engagement, and systematically terminating the session based on it. If the cause is fatigue,
620 giving the animals a “rest period” might help. Alternatively, our task can be implemented in animal’s
621 home cage so that the data can be collected in a self-paced condition for a much longer time (e.g. (Poddar
622 et al., 2013)). Third, adding cue-only trials (in which the auditory cue is played but the perturbation is
623 omitted) would be important to further investigate the biological process of how the cue induces the
624 beneficial effect on postural responses. If the cue itself is enough to elicit postural responses without an
625 actual perturbation, this would provide strong support for associative learning(Campbell et al., 2009).

626 Although the mouse model is powerful because of its compatibility with techniques for recording
627 and manipulating neural activities, it is crucial to note the differences between our mouse paradigm and

human paradigms that stem from the nature of the species. Notably, musculoskeletal structure differences such as tail, segment alignment, and body mass proportions impact balance dynamics. Tails could contribute to balance in several different ways: 1) The tail movements can have a positive influence on the whole-body center of mass; 2) It can generate torque, partially compensating for that generated by gravity (similar to how arm-reaching can affect balance in humans(Muehlbauer et al., 2022)); If the tail is touching the floor, 3) the external force from the floor might mechanically affect balance; 4) it widens the base of support and increases stability; and 5) it produces sensory feedback by touch. Our observations indicate that mice often touch the floor with their tails instead of keeping them in the air during quiet bipedal standing and that the tails make dynamic movements during the perturbation. Therefore, tethering the tail and measuring the force applied by the tail(Funato et al., 2017) might be necessary, to dissect out the mechanical contributions of different body parts other than the tail to balance. Additionally, differences in segment alignment and body mass proportions between mice and humans underscore the need for careful consideration in comparative research. A mouse is a quadrupedal animal, and its body is not adapted to maintaining an upright posture for a long time. (It should be noted, though, that rearing up on the hind legs is a part of the murine repertoire of natural behavior related to exploration(Sturman et al., 2018).) It has been shown that body segments of rats during quiet bipedal standing are comparable but flexed compared to those of humans which are nearly aligned(Funato et al., 2017). In the study that explored bipedal rats' postural responses to the backward rotation of the floor, the researchers showed that the postural responses were generally common between humans and rats but found the bending of the trunk in rats as a response to the floor rotation, which is not commonly observed in humans(Konosu et al., 2021). They suggested that this might be due to the mass and length of the trunk accounting for a greater proportion of the rat's whole body compared to humans, as well as the aforementioned alignment differences. While our analysis did not encompass segment kinematics, we anticipate similar segment alignment and body mass proportions in mice as observed in rats. These differences are important to keep in mind but do not necessarily diminish the importance of our findings and their connections to human studies. Bipedal standing in mice is intrinsically unstable and would thus require stabilization by a neural control system. Leveraging the mouse model's genetic tools and neural recording/manipulation techniques can elucidate the neural mechanisms underlying postural control, offering insights relevant to human studies.

It is also important to note the differences between our mouse paradigm and human paradigms that arise from the design of experiments in addition to the musculoskeletal differences mentioned above. The control of the pre-perturbation posture is one of such key differences between mouse and human paradigms. Unlike human tasks, where participants assume specific postures and remain still before perturbation, controlling pre-perturbation posture in mice to the same extent is challenging. Moreover,

mice must continue licking to keep the trial active, impacting their pre-perturbation posture. While we utilized a perch to restrict standing orientation and positions, variability in pre-perturbation postures, including movements of feet, arms, and tail, was observed. Therefore, it is important to keep in mind that the pre-perturbation posture could be affecting the postural responses to the perturbation.

The potential for further advancement and application of this study lies in the deeper understanding of posture control dynamics through more extensive analysis of both kinematics and kinetics, as well as in the elucidation of neural circuits through experiments using electromyography (EMG), neural recording, and neural manipulation techniques. Further study on kinematics could include center of mass analysis that is often used in human postural studies(Peterka, 2002; Ting, 2007; Van Wouwe et al., 2021; Welch and Ting, 2014), three-dimensional kinematic analysis integrating data from multiple cameras(Dunn et al., 2021; Karashchuk et al., 2021; Marshall et al., 2020; Nath et al., 2019), and unsupervised clustering of recorded movements(Marshall et al., 2020; Wiltschko et al., 2020, 2015) to uncover novel postural and kinematic strategies including pre-perturbation kinematic changes. In addition, EMG recordings and force measurements on the perch would be useful additions to our paradigm in order to detect postural adjustments that are not reflected in kinematics such as muscle co-contraction or toe gripping on the perch.

Potential neural experiments could include systematic neural manipulations and invasive measurement methods that provide improved temporal and spatial resolution along with the capability to manipulate or record specific types of neurons or neurons within a specific circuit using genetic tools(Roth, 2016; Tsai et al., 2009; Zariwala et al., 2012; Zhang et al., 2010) and tracing technology(Tervo et al., 2016; Wickersham et al., 2007). One can generate specific hypotheses on the functions of neural signals and test those with more specific neural intervention methods such as optogenetics, which can influence specifically targeted neurons in a temporally precise manner(Tsai et al., 2009; Zhang et al., 2010). It might be possible to find a specific manipulation that could eliminate or impair one aspect of predictive postural control without degrading other aspects. For example, after the cue-perturbation association is established, one could perform optogenetic manipulation selectively during the cue period to test whether the performance difference between cued and uncued conditions decreased while the overall postural performance was maintained. Recent advances in wireless optogenetics methods have the potential to greatly facilitate these experiments in freely moving animals(Nourizonoz et al., 2020; Yang et al., 2021).

To conclude, we have established a mouse experimental paradigm with which to explore the neural mechanisms underpinning predictive postural control. Neural mechanisms underlying postural control are understudied compared to movement controls, let alone the kind of predictive postural control

studied in this work. Technological developments in computer vision and machine learning now provide us with a tremendous opportunity to fully explore the complexity of free and whole-body movements. Concurrently, neuroscience tools available in mice give us leverage to elucidate the neural mechanisms underpinning predictive postural control. Our work establishes a mouse experimental paradigm to study predictive postural control and opens the door to the circuit-level understanding of its underlying mechanisms.

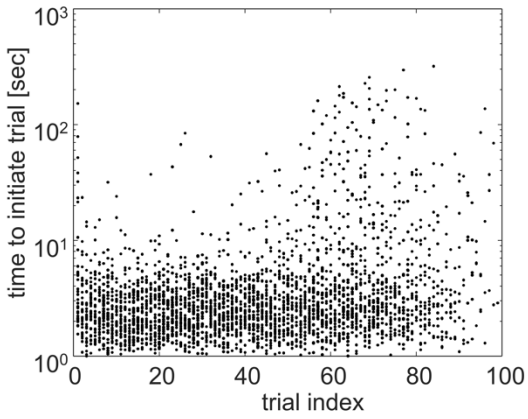

Figure 8: Time to initiate trial
Time to initiate the trial for each trial from sessions in which this information was available (all sessions for CB5 and CB6, session #1-5 for CB10) from all three mice are superimposed. Note that each session has a different number of trials. Trials in which the time to initiate is shorter than 1 sec are rare and omitted from this plot.

Acknowledgments

We thank Akira Konosu and all Uchida and Yanagihara lab members for their discussion and feedback. We also would like to acknowledge the support of Ed Soucy, Brett Graham, and the Center for Brain Science Neurotechnology Core for their help in building the experimental apparatus, and Kohei Yamaji for his help in illustrations. This work was supported by the Simons Collaboration of the Global Brain (N.U.), Grants-in-Aid for for Scientific Research (C) (18K10955) funded by the Ministry of Education, Culture, Sports, Science, and Technology of Japan (D.Y.), Murata Overseas Scholarship (Y.D.), and Masason Foundation (Y.D.).

References

Allen NE, Canning CG, Almeida LRS, Bloem BR, Keus SH, Löfgren N, Nieuwboer A, Verheyden GS, Yamato TP, Sherrington C (2022) Interventions for preventing falls in Parkinson's disease. Cochrane Database Syst Rev 6:CD011574.

Bastian AJ (2006) Learning to predict the future: the cerebellum adapts feedforward movement control. Curr Opin Neurobiol 16:645–649.

Berridge KC (2004) Motivation concepts in behavioral neuroscience. Physiol Behav 81:179–209.

Campbell AD, Dakin CJ, Carpenter MG (2009) Postural responses explored through classical conditioning. Neuroscience 164:986–997.

CDC Older Adult Falls [WWW Document] (2023). URL https://www.cdc.gov/falls/index.html (accessed 3.6.24).

Coelho DB, Luis ·., Teixeira A (2017) Cognition and balance control: does processing of explicit contextual cues of impending perturbations modulate automatic postural responses? Exp Brain Res 235:2375–2390.

Dakin CJ, Bolton DAE (2018) Forecast or Fall: Prediction's Importance to Postural Control. Front Neurol 9:924.

Denissen S, Staring W, Kunkel D, Pickering RM, Lennon S, Geurts AC, Weerdesteyn V, Verheyden GS (2019) Interventions for preventing falls in people after stroke. Cochrane Database Syst Rev 10:CD008728.

Dunn TW, Marshall JD, Severson KS, Aldarondo DE, Hildebrand DGC, Chettih SN, Wang WL, Gellis AJ, Carlson DE, Aronov D, Freiwald WA, Wang F, Ölveczky BP (2021) Geometric deep learning enables 3D kinematic profiling across species and environments. Nat Methods 18:564–573.

Fujio K, Obata H, Kawashima N, Nakazawa K (2016) The effects of temporal and spatial predictions on stretch reflexes of ankle flexor and extensor muscles while standing. PLoS One 11.

Funato T, Sato Yota, Fujiki S, Sato Yamato, Aoi S, Tsuchiya K, Yanagihara D (2017) Postural control during quiet bipedal standing in rats. PLoS One 12.

Horak FB, Diener HC (1994) Cerebellar control of postural scaling and central set in stance. J Neurophysiol 72:479–493.

Horak FB, Diener HC, Nashner LM (1989) Influence of central set on human postural responses. J Neurophysiol 62:841–853.

Horak FB, Nashner LM (1986) Central programming of postural movements: adaptation to altered support-surface configurations. J Neurophysiol 55:1369–1381.

Jacobs JV, Fujiwara K, Tomita H, Furune N, Kunita K, Horak FB (2008) Changes in the activity of the cerebral cortex relate to postural response modification when warned of a perturbation. Clin Neurophysiol 119:1431–1442.

Jacobs JV, Horak FB (2007) Cortical control of postural responses. J Neural Transm 114:1339–1348.

Kannus P, Sievänen H, Palvanen M, Järvinen T, Parkkari J (2005) Prevention of falls and consequent injuries in elderly people. Lancet 366:1885–1893.

Karashchuk P, Rupp KL, Dickinson ES, Walling-Bell S, Sanders E, Azim E, Brunton BW, Tuthill JC (2021) Anipose: A toolkit for robust markerless 3D pose estimation. Cell Rep 36:109730.

Kolb FP, Lachauer S, Maschke M, Timmann D (2004) Classically conditioned postural reflex in cerebellar patients. Exp Brain Res 158:163–179.

Kolb FP, Lachauer S, Maschke M, Timmann D (2002) Classical conditioning of postural reflexes. Pflugers Arch 445:224–237.

Kolb FP, Timmann D, Baier PC, Diener HC (2000) Classically conditioned withdrawal reflex in cerebellar patients. 2. Impaired unconditioned responses. Exp Brain Res 130:471–485.

Konosu A, Funato T, Matsuki Y, Fujita A, Sakai R, Yanagihara D (2021) A Model of Predictive Postural Control Against Floor Tilting in Rats. Front Syst Neurosci 15:785366.

Konosu A, Matsuki Y, Fukuhara K, Funato T, Yanagihara D (2024) Roles of the cerebellar vermis in predictive postural controls against external disturbances. Sci Rep 14:3162.

Lauer J, Zhou M, Ye S, Menegas W, Schneider S, Nath T, Rahman MM, Di Santo V, Soberanes D, Feng G, Murthy VN, Lauder G, Dulac C, Mathis MW, Mathis A (2022) Multi-animal pose estimation, identification and tracking with DeepLabCut. Nat Methods 19:496–504.

Lockhart DB, Ting LH (2007) Optimal sensorimotor transformations for balance. Nat Neurosci 10:1329–1336.

Marshall JD, Aldarondo DE, Dunn TW, Wang WL, Berman GJ, Ölveczky BP (2020) Continuous Whole-Body 3D Kinematic Recordings across the Rodent Behavioral Repertoire. Neuron.

Massion J (1992) Movement, posture and equilibrium: interaction and coordination. Prog Neurobiol 38:35–56.

769 Mathis A, Mamidanna P, Cury KM, Abe T, Murthy VN, Mathis MW, Bethge M (2018) DeepLabCut: markerless
770 pose estimation of user-defined body parts with deep learning. Nat Neurosci 21:1281–1289.
771 McChesney JW, Sveistrup H, Woollacott MH (1996) Influence of auditory precuing on automatic postural
772 responses. Exp Brain Res 108:315–320.
773 Mochizuki G, Sibley KM, Esposito JG, Camilleri JM, McIlroy WE (2008) Cortical responses associated with the
774 preparation and reaction to full-body perturbations to upright stability. Clin Neurophysiol 119:1626–1637.
775 Muehlbauer T, Hill MW, Heise J, Abel L, Schumann I, Brueckner D, Schedler S (2022) Effect of Arm Movement
776 and Task Difficulty on Balance Performance in Children, Adolescents, and Young Adults. Front Hum
777 Neurosci 16:854823.
778 Nashner LM, Cordo PJ (1981) Relation of automatic postural responses and reaction-time voluntary movements of
779 human leg muscles. Exp Brain Res 43:395–405.
780 Nath T, Mathis A, Chen AC, Patel A, Bethge M, Mathis MW (2019) Using DeepLabCut for 3D markerless pose
781 estimation across species and behaviors. Nat Protoc 14:2152–2176.
782 Nourizonoz A, Zimmermann R, Ho CLA, Pellat S, Ormen Y, Prévost-Solié C, Reymond G, Pifferi F, Aujard F,
783 Herrel A, Huber D (2020) EthoLoop: automated closed-loop neuroethology in naturalistic environments.
784 Nat Methods 17:1052–1059.
785 Ortiz AV, Aziz D, Hestrin S (2020) Motivation and Engagement during Visually Guided Behavior. Cell Rep
786 33:108272.
787 Peterka RJ (2002) Sensorimotor integration in human postural control. J Neurophysiol 88:1097–1118.
788 Poddar R, Kawai R, Ölveczky BP (2013) A fully automated high-throughput training system for rodents. PLoS One
789 8:e83171.
790 Pruszynski JA, Scott SH (2012) Optimal feedback control and the long-latency stretch response. Exp Brain Res
791 218:341–359.
792 Roth BL (2016) DREADDs for Neuroscientists. Neuron 89:683–694.
793 Santos MJ, Kanekar N, Aruin AS (2010) The role of anticipatory postural adjustments in compensatory control of
794 posture: 1. Electromyographic analysis. J Electromyogr Kinesiol 20:388–397.
795 Schepens B, Drew T (2004) Independent and convergent signals from the pontomedullary reticular formation
796 contribute to the control of posture and movement during reaching in the cat. J Neurophysiol 92:2217–
797 2238.
798 Silva MB, Coelho DB, de Lima-Pardini AC, Martinelli AR, Baptista T da S, Ramos RT, Teixeira LA (2015)
799 Precueing time but not direction of postural perturbation induces early muscular activation: Comparison
800 between young and elderly individuals. Neurosci Lett 588:190–195.
801 Sturman O, Germain P-L, Bohacek J (2018) Exploratory rearing: a context- and stress-sensitive behavior recorded in
802 the open-field test. Stress 21:443–452.
803 Tervo DGR, Hwang B-Y, Viswanathan S, Gaj T, Lavzin M, Ritola KD, Lindo S, Michael S, Kuleshova E, Ojala D,
804 Huang C-C, Gerfen CR, Schiller J, Dudman JT, Hantman AW, Looger LL, Schaffer DV, Karpova AY
805 (2016) A Designer AAV Variant Permits Efficient Retrograde Access to Projection Neurons. Neuron
806 92:372–382.
807 Ting LH (2007) Dimensional reduction in sensorimotor systems: a framework for understanding muscle
808 coordination of posture. Prog Brain Res 165.
809 Tsai H-C, Zhang F, Adamantidis A, Stuber GD, Bonci A, de Lecea L, Deisseroth K (2009) Phasic firing in
810 dopaminergic neurons is sufficient for behavioral conditioning. Science 324:1080–1084.
811 Van Wouwe T, Ting LH, De Groote F (2021) Interactions between initial posture and task-level goal explain
812 experimental variability in postural responses to perturbations of standing balance. J Neurophysiol
813 125:586–598.
814 Wei WE, De Silva DA, Chang HM, Yao J, Matchar DB, Young SHY, See SJ, Lim GH, Wong TH,
815 Venketasubramanian N (2019) Post-stroke patients with moderate function have the greatest risk of falls: a
816 National Cohort Study. BMC Geriatr 19:373.
817 Welch TDJ, Ting LH (2014) Mechanisms of motor adaptation in reactive balance control. PLoS One 9:e96440.
818 Wickersham IR, Lyon DC, Barnard RJO, Mori T, Finke S, Conzelmann K-K, Young JAT, Callaway EM (2007)
819 Monosynaptic restriction of transsynaptic tracing from single, genetically targeted neurons. Neuron
820 53:639–647.
821 Wiltschko AB, Johnson MJ, Iurilli G, Peterson RE, Katon JM, Pashkovski SL, Abraira VE, Adams RP, Datta SR
822 (2015) Mapping Sub-Second Structure in Mouse Behavior. Neuron 88:1121–1135.

Wiltschko AB, Tsukahara T, Zeine A, Anyoha R, Gillis WF, Markowitz JE, Peterson RE, Katon J, Johnson MJ, Datta SR (2020) Revealing the structure of pharmacobehavioral space through motion sequencing. Nat Neurosci 23:1433–1443.

Wolpert DM, Flanagan JR (2001) Motor prediction. Curr Biol 11:R729-32.

Yang Y et al. (2021) Wireless multilateral devices for optogenetic studies of individual and social behaviors. Nat Neurosci 24:1035–1045.

Zariwala HA, Borghuis BG, Hoogland TM, Madisen L, Tian L, De Zeeuw CI, Zeng H, Looger LL, Svoboda K, Chen T-W (2012) A Cre-dependent GCaMP3 reporter mouse for neuronal imaging in vivo. J Neurosci 32:3131–3141.

Zhang F, Gradinaru V, Adamantidis AR, Durand R, Airan RD, de Lecea L, Deisseroth K (2010) Optogenetic interrogation of neural circuits: technology for probing mammalian brain structures. Nat Protoc 5:439–456.